Combustion Chamber Wall Temperature Measurement and Modeling During Transient HCCI Operation

Wilhelmsson, Carl; Vressner, Andreas; Tunestål, Per; Johansson, Bengt; Särner, Gustaf; Aldén, Marcus

2005

2005-01-3731

Combustion Chamber Wall Temperature Measurement and Modeling During Transient HCCI Operation

Carl Wilhelmsson, Andreas Vressner, Per Tunestål and Bengt Johansson
Division of Combustion Engines, Lund Institute of Technology

Gustaf Särner, Marcus Aldén
Division of Combustion Physics, Lund Institute of Technology

ABSTRACT

In this paper the combustion chamber wall temperature was measured by the use of thermographic phosphor. The temperature was monitored over a large time window covering a load transient.

Wall temperature measurement provide helpful information in all engines. This temperature is for example needed when calculating heat losses to the walls. Most important is however the effect of the wall temperature on combustion. The walls can not heat up instantaneously and the slowly increasing wall temperature following a load transient will affect the combustion events sucseeding the transient. The HCCI combustion process is, due to its dependence on chemical kinetics more sensitive to wall temperature than Otto or Diesel engines. In depth knowledge about transient wall temperature could increase the understanding of transient HCCI control.

A “black box” state space model was derived which is useful when predicting transient wall temperature. To produce a model the engine is run with the load described by a Pseudo Random Binary Sequence (PRBS). Standard system identification methodology was then applied to acquire a state space model which calculate the combustion chamber wall temperature given $IMEP_n$. Such a model is useful when controlling HCCI combustion and makes it possible to compensate the impact of wall temperature delay following a load transient.

INTRODUCTION

The HCCI engine is still less known than its relatives the Otto and the Diesel engine. Never the less it seems to be one of the most promising engine concepts of the future, combining high efficiency with ultra low emissions of the unwanted nitrogen oxides. The first report of the concept of HCCI combustion was presented by Onishi et al. [1] and was initially primarily an attempt to reduce emissions of unburned hydrocarbons (HC) and improve part load efficiency for two stroke engines. The working principle of the HCCI engine is best understood as a hybrid between the Otto and Diesel engines. The HCCI engine operates with a premixed charge as in the Otto engine, and it operates unthrottled with compression ignition, controlling the load via the global air/fuel equivalence ratio (lambda) like the diesel engine. This operation principle makes it possible to increase the efficiency compared to the Otto engine due to the avoidance of throttling losses. At the same time the high soot and nitrogen oxide emissions of the diesel engine are avoided. Soot emissions is avoided bechause of the homoginety of the mixture and the avoidance of localy rich combustion zones. Nitrogen oxide emissions on the other hand is avoided because of the decrease in peak in-cylinder temperature due to the lean operation of the engine.

HCCI combustion can be achieved in numerous ways, both in two and four stroke engines. The compression ratio can be increased, the inlet air can be pre heated, the HCCI combustion can be triggered by the use of retained hot residual gas and the octane number of the fuel can be altered [2]-[8]. Since

the HCCI combustion process is very sensitive to numerous parameters, feedback combustion control is needed to operate an HCCI engine in parts of its operation range as shown by Olsson et al. [14]. Such combustion control can be performed in numerous ways using different actuators [10]-[13].

Even though it has many good features, the HCCI engine also has some limitations. The operational principle unfortunately suffers from very high combustion rates. This high combustion rate causes noise as well as wear of engine hardware. Another problem with the HCCI principle is low combustion efficiency at low load. This causes high emissions of unburned hydrocarbons and carbon monoxide [9]. The lower exhaust temperature will cause problems when trying to fit a catalytic converter to an HCCI engine.

One of the factors that affects HCCI combustion is combustion chamber wall temperature. The HCCI combustion is as shown by Olsson et al. [14] very sensitive to the temperature history of the engine; this paper focuses on the behavior of the wall temperature when a sudden change of engine load (a load transient) occurs. Investigations of the wall temperature behaviour of an HCCI engine have previously been performed by the use of thermocouples by Chang et al. [15]. Chang however focuses on the wall temperature as it is changing within the engine cycle and the main purpose is the development of a heat transfer model suitable for HCCI engines. The conducted work has focused on how the wall temperature changes from cycle to cycle when the HCCI engine is exposed to an increase in load.

The technique used to measure wall temperature is called Laser Induced Phosphorescence (LIP) and has previously been used to measure temperatures in internal combustion engines [16]-[19]. The LIP technique has the advantage that it measures the temperature almost intrinsically. It is also possible to measure temperature remotely using the LIP technique. The down side with this technique is that optical access has to be provided to the measurement spot.

To improve transient HCCI control a model describing wall temperature is very useful. The output of the model can be used for feed-forward action in the controller structure compensating for the effects that wall temperature has on the combustion [24]. Such a model has the potential to significantly simplify the combustion feedback controller needed to operate an HCCI engine. A model describing wall temperature was identified using standard system identification techniques [22]. The engine was run on a load described by a Pseudo Random Binary Sequence (PRBS) and wall temperature was measured. From the measured wall temperature and IMEP a wall temperature model was identified using the subspace algorithm [23]. The model performance was cross validated by the use of data not used in the identification process.

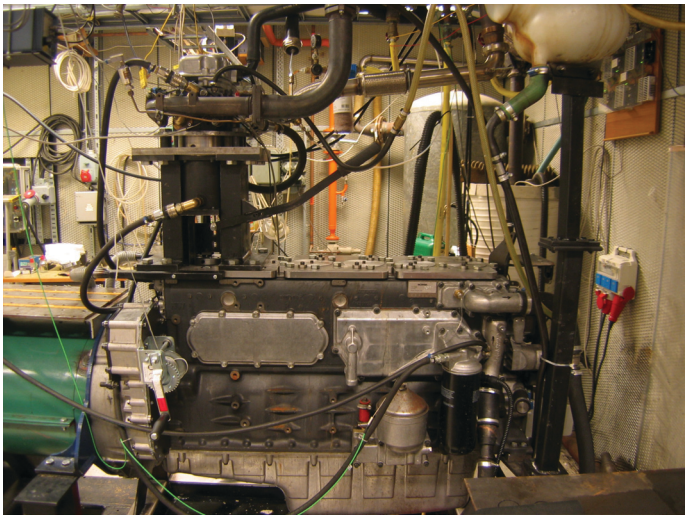

Figure 1: The test engine used in the experiments.

Table 1: Engine geometric properties.

Displaced Volume	1966 cm^3
Bore	127.5 mm
Stroke	154 mm
Connecting Rod Length	255 mm
Number of Valves	4
Compression Ratio	16.0:1
Exhaust valve open	$34\,^\circ$ BBDC @ 0.15 mm
Exhaust valve close	$6\,^\circ$ BTDC @ 0.15 mm
Exhaust valve lift	14.1 mm
Exhaust valve diameter	41 mm
Inlet valve open	$2\,^\circ$ BTDC @ 0.15 mm
Inlet valve close	$29\,^\circ$ ABDC @ 0.15 mm
Inlet valve lift	14.1 mm
Inlet valve diameter	45 mm
Fuel Supply	PFI

EXPERIMENTAL APPARATUS

EXPERIMENTAL ENGINE The engine used in the conducted experiments was a 12l Scania heavy duty diesel engine converted to single-cylinder HCCI operation. The engine is fitted with a piston glass and a piston extension to enable optical access from underneath the glass piston. With the help of a mirror it is possible to lead laser pulses through the piston glass and the combustion chamber to the cylinder head. Besides the piston glass no other glass walls are present in the engine; all the other combustion chamber walls consist of metal.

CONTROL SOFTWARE The engine was operated manually without feedback combustion control. Injection control software was however used to control the injection timing and other important operational parameters such as inlet temperature. The control software is basically a variant of the system presented by Olsson et al. [10], modified to fit the single-cylinder engine used. The feedback controllers featured in the software are switched off and no feedback control of the combustion is applied. Prior to these experiments, functionality was added to enable a PRBS disturbance on the total fuel heat feed in each injection. The PRBS sequence provides the possibility to perform system identification and obtain a dynamic state space model of the wall temperature as a function of the IMEP$_n$ time history.

TEMPERATURE MEASUREMENT

LIP, LASER INDUCED PHOSPHORESCENCE
Laser Induced Phosphorescence (LIP) is a technique where phosphorescence from thermographic phosphors is utilized for determination of temperature. Wall temperature measurement can be made from room temperature up to 2000 K, remotely, close to non-intrusively and with high accuracy as shown by Allison et al. [20]. The lifetime, i.e. the time for the phosphorescence intensity to decrease to $1/e$ of its original intensity, is temperature dependent for thermographic phosphors and can be calibrated to provide absolute temperature readings.

In this work the thermographic phosphor La_2O_2S:Eu was used for its temperature sensitivity in the region of interest, 150 - 300 C. The lifetime of its phosphorescence was calibrated to temperature in a controlled environment before the measurements. The phosphor was painted as a spot on the cylinder head, the binder used was HPC. The spot was positioned close to the hole originally used by the diesel fuel injector on the side facing the exhaust valves. No cooling water or oil channels are present in the direct vicinity of the phosphor spot.

The phosphor spot was excited by 355 nm laser UV-light produced by a pulsed Nd:YAG-laser working at its third harmonic. The pulsed 10 Hz laser light was directed to the phosphor spot via the 45° mirror below the piston window as shown in Figure 2. The emission signal was collected by a quartz glass lens with f = +100 mm and d = 50 mm and focused on the Photo Multiplier Tube (PMT). An interference filter centered at 538 nm was placed in front of the PMT for spectral filtering to the spectral line of interest. The amplified signal from the PMT was sampled and

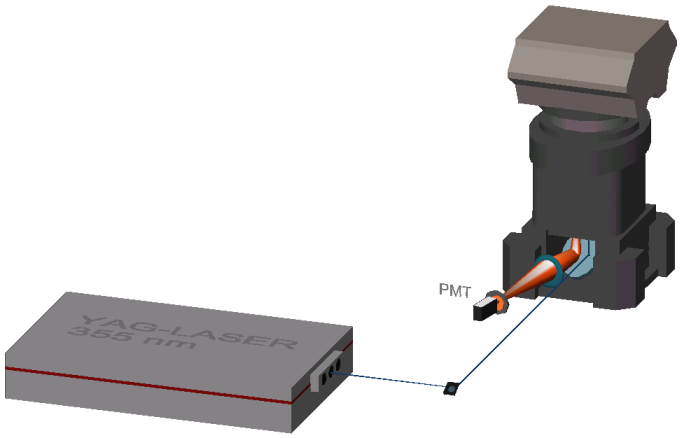

Figure 2: Laser based temperature measurement setup.

saved by a LeCroy 3 GHz oscilloscope.

This temperature measurement methodology has previously been performed in a single cylinder HD Diesel engine running under partly premixed conditions by Husberg et al. [17]; they however measured the temperature on the piston top evaluating different methods to solve the optical access and comparing this technique with the conventional thermocouples.

LIP MEASUREMENT ACCURACY The accuracy of the LIP temperature measurement technique is according to Childes et al. [21] estimated to 1%, which in this case means an accuracy in the range of 1.5-2 °C. The standard deviation of the measured temperature was by Särner et al. [16] found to be 0.73 °C at 57 CAD BTDC. Since the temperature measurements are performed at 50 CAD BTDC the standard deviation is probably slightly higher than 0.73 °C, but it is still below 1 °C.

Note that the selected timing of the wall temperature measurement (50 CAD BTDC) is used since it is within a crank angle interval found by Särner et al. [16] to show very low variance between the cycles, this to suppress the effect of the cyclic variability. The cyclic variability has its lowest impact if the wall temperature measurements are performed somewhere between 47 and 67 CAD BTDC. The objective in this study is not to investigate the cyclic variability of the wall temperature and hence the timing with least sensitivity to cyclic variability is selected.

TEST PROCEDURE

In all these tests the engine was run using pure isooctane as fuel. When performing the tests the engine was first started up and run in steady state for quite

some time. When the engine finally reached thermal equilibrium the transient tests were carried out. A typical step was performed in the manner that the engine was first run in steady state for a short while. The laser and the data collection systems were started, to get a well defined output intensity from the laser the transient was not started until at least 20 s after the laser was started. The injected total fuel heat was then drastically increased. Since the change in fuel heat can be considered to have changed between cycles IMEP$_n$ can also be considered to have done so. There will of course be a latency due to inlet port wetting. This latency is however evidently very small considering the time it takes the wall temperature to respond to the load change. The engine was then run until the desired number of cycles had been captured.

The laser setup was synchronized with the engine data acquisition system and it should be pointed out that the measured temperatures were synchronized with the corresponding engine cycles. Since the engine is run at 1200rpm the engine performs 10 cycles each second. This means that even though the temperature often is presented time based it is synchronized with IMEP$_n$ which is presented cycle based.

EXPERIMENTAL RESULTS

STEP DISTURBANCE The first reasonable investigation to carry out is an investigation of the response of the wall temperature. The pure step disturbance gives an answer about the rise time of the wall temperature and it basically gives the answer to the response of the combustion chamber walls to that particular transient. It is important to remember that the experiments are carried out on an optical engine run at moderate loads and a fixed engine speed of 1200rpm to match the 10Hz pulsation of the laser. The wall temperature can be expected to be higher in an all metal engine running at higher loads. It is difficult however to make a general statement regarding the difference in thermal inertia between an optical engine and an all metal engine. The thermal inertia is likely to depend on the design of the combustion chamber cooling system and so on. It hence probably differs substantially between different engines.

POSITIVE STEP DISTURBANCE Figure 3 shows the IMEP$_n$ corresponding to a representative single positive step disturbance. Figure 4, Figure 5 and Figure 6 show the calculated combustion phasing , calculated combustion duration and measured wall temperature. As seen in the figures the walls, as expected respond very slowly to the sudden increase

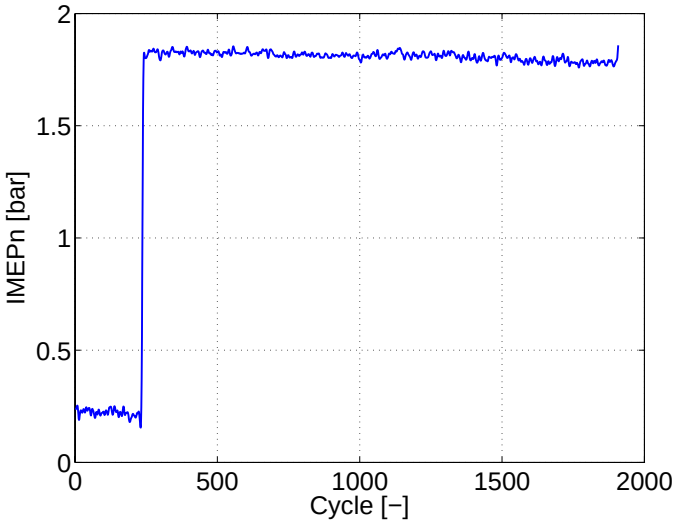

Figure 3: A positive step disturbance of IMEP$_n$.

in IMEP$_n$. Note that IMEP$_n$, combustion duration and combustion phasing are filtered.

The rise time (10%-90%) of the temperature in Figure 6 is found to be about 110 seconds (1100 cycles as the engine is run at 1200 rpm). The average rise time considering the five different available positive step disturbances is 108 seconds. There exists a slight spread in the temperature which is a result of cycle to cycle variations of the combustion process. When investigating combustion phasing and duration (Figure 4 and Figure 5) we realize that combustion duration decreases significantly after the load disturbance has occurred, the combustion also takes place earlier in the cycle. Initially however the sudden increase in the fuel amount feed to the engine retards CA50 due to the fuel vaporization-related decrease of charge temperature. CA50 then occurs earlier and earlier as the walls (and engine as such) heat up. The fact that CA50 initially occurs later affects combustion duration which is increased, some cycles completely misfire because of the late combustion phasing. When CA50 advances beyond its previous “steady state” value of 6 CAD the occasional misfiring ends. After the initial steep decrease of combustion duration it is easily noticed that combustion duration slowly decreases as the wall temperature increases and as the combustion phasing advances ever further. The misfiring due to late combustion phasing can not be seen in Figure 3 because of the filtering applied to the data presented in this figure.

NEGATIVE STEP DISTURBANCE A question that arises when investigating the positive step disturbance (Figure 3 and Figure 6) is if the fall time of the wall temperature equals the rise time. The investigation is performed in the same manner as the

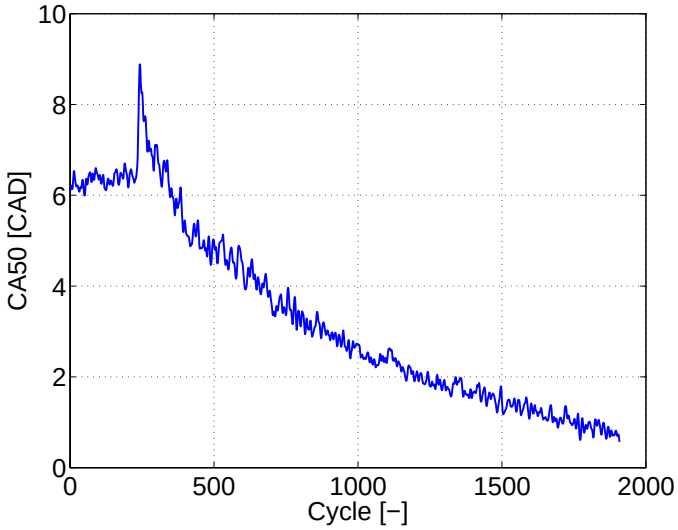

Figure 4: CA50 (CAD ATDC) corresponding to Figure 3.

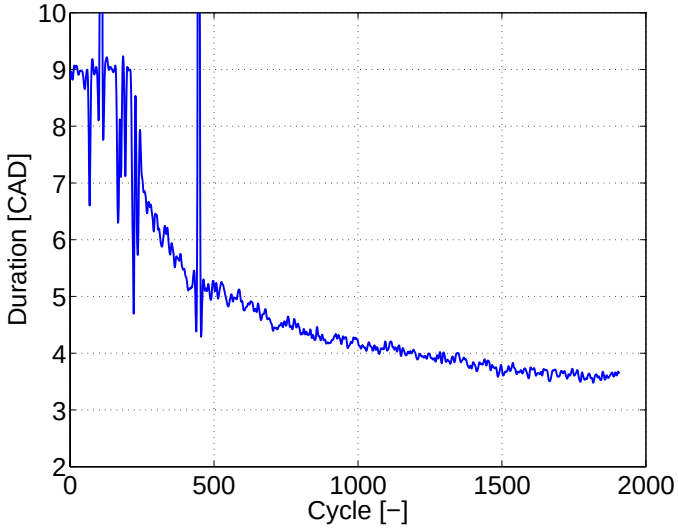

Figure 5: Combustion duration corresponding to Figure 3.

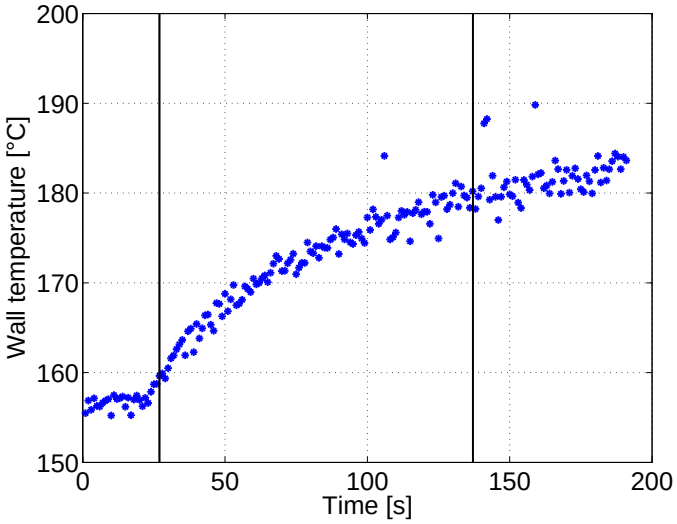

Figure 6: The temperature corresponding to the step disturbance shown in Figure 3.

investigation of the positive step response. When this is done we realize that the fall time has the same mean average value as the rise time. The average value of both the rise time and the fall time is 108 seconds

Even though the wall temperature needs the same time to stabilize both after the positive and the negative step disturbances, the combustion phasing and duration behave totally different. The wall temperature are about to decrease and we realize from Figure 8, Figure 9 and Figure 10 that the latency of the wall temperature affects the combustion less than it did in the case with the positive step disturbance. This seems surprising but when the fuel heat decreases there is no extra cooling due to fuel vaporization. Combustion phasing does not change very dramatically, it initially changes rapidly about one CAD because of the sudden change of lambda. However as the wall temperature decreases the combustion occurs later and later in the cycle and CA50 (almost) stabilizes at around 4 CAD ATDC.

Onset of HCCI combustion is governed by chemical kinetics which in turn depends strongly on temperature and this explains why the combustion phasing changes substantially as the wall temperature decreases. The combustion duration is mostly limited by the current lambda which is changed instantaneously when the fuel heat is decreased. Since current air/fuel ratio limits the combustion duration the wall temperature only slightly affects the combustion duration as the walls cool off and the combustion phasing occurs later. Hence there is only a barely visible increase of the combustion duration after the initial instantaneous change.

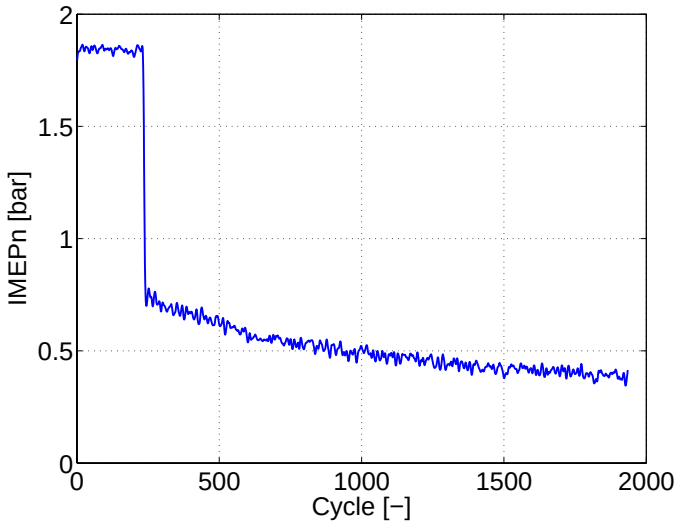

Figure 7: A negative step disturbance of IMEP$_n$.

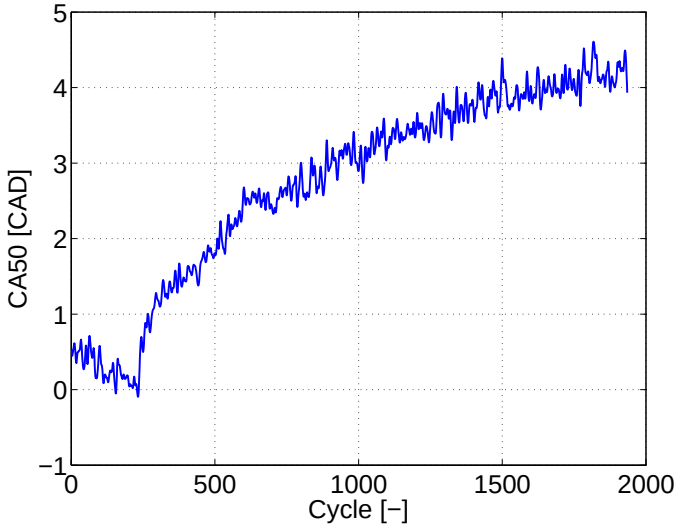

Figure 8: CA50 (CAD ATDC) corresponding to Figure 7.

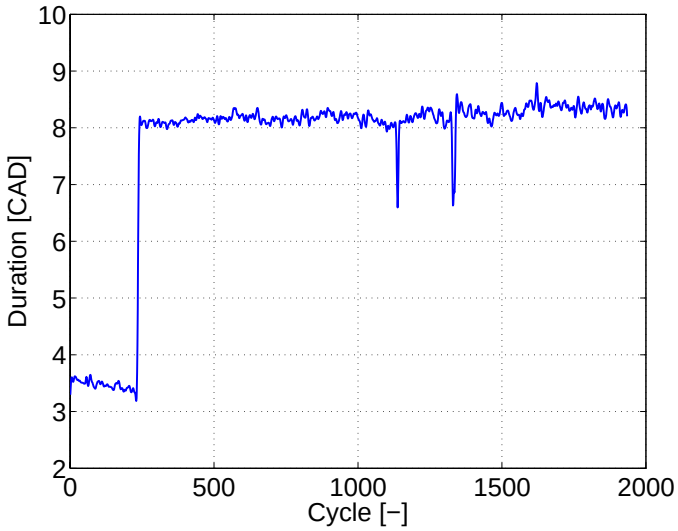

Figure 9: Combustion duration corresponding to Figure 7.

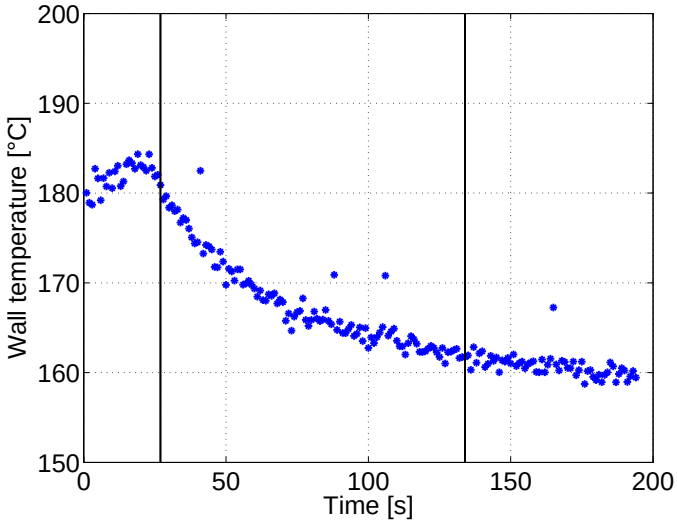

Figure 10: The temperature corresponding to the step disturbance shown in Figure 7.

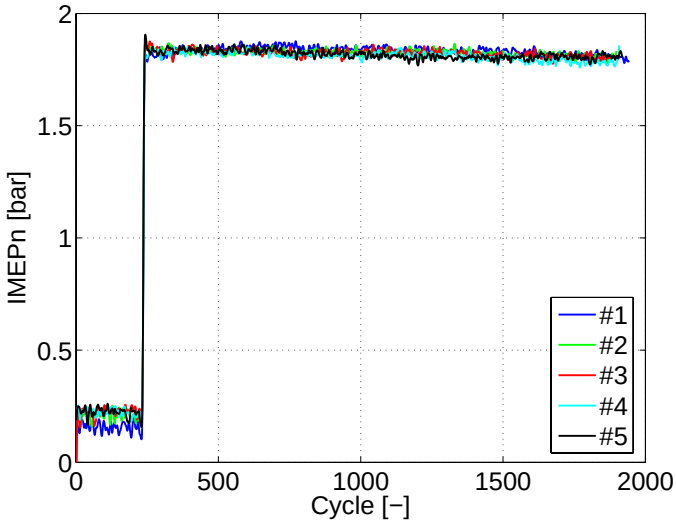

Figure 11: Repeated positive IMEP$_n$ step disturbance.

REPEATABILITY To confirm that the acquired temperature is valid, it is essential to be able to repeat the behaviour on several different occasions. To realize the repeated steps the actual combustion duration was manually monitored and the measurement was started when the combustion duration had approximately the same value. The different transients were aligned to be able to put them on top of each other in one single figure. Five different positive step disturbances are shown in Figure 11 and as seen the behaviour on the different occasions is identical. This statement is also valid for the repeated negative step disturbances shown in Figure 13. Clearly visible is also the fact that the rise/fall time is equal, and around 110 seconds (1100 cycles). Both combustion phasing and combustion duration are also repetitive in their character.

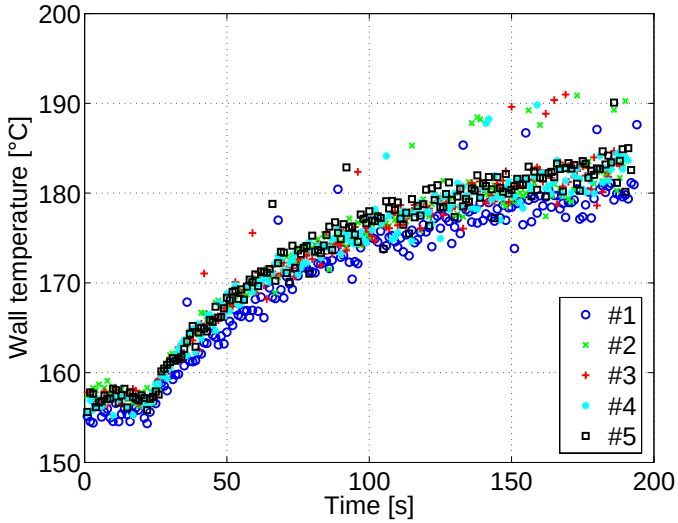

Figure 12: Temperatures corresponding to Figure 11.

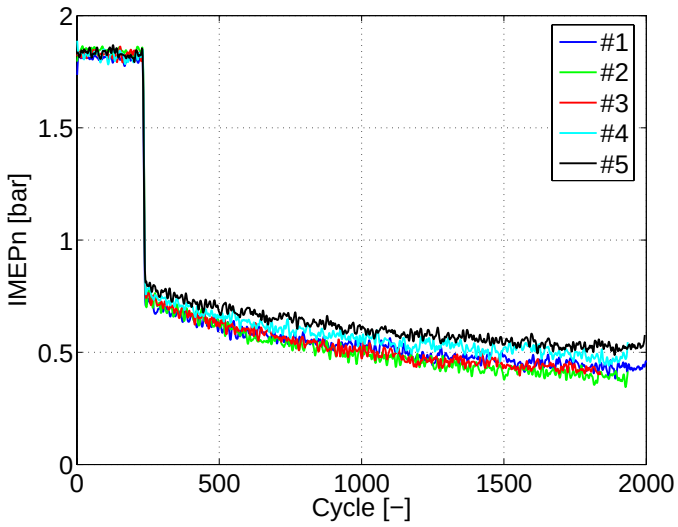

Figure 13: Repeated negative IMEP$_n$ step disturbance.

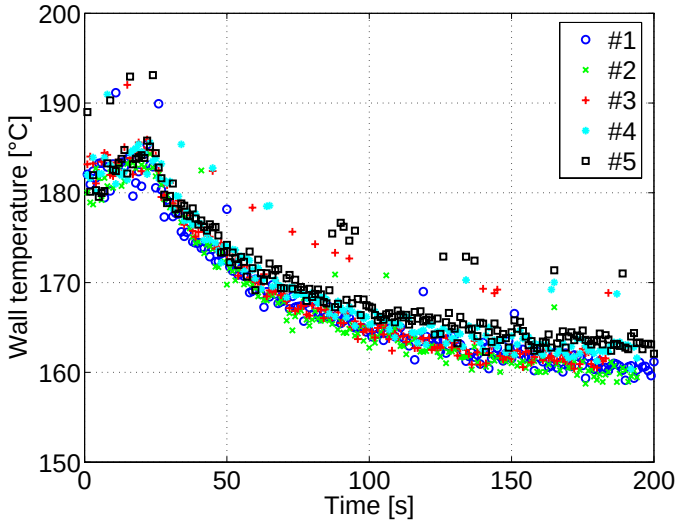

Figure 14: Temperatures corresponding to Figure 13.

COMBUSTION INSTABILITY In Figure 6 it is noticeable that the temperature never reaches a stable steady state; we hence have a slightly unstable system. The lack of feedback combustion control makes it impossible to break the instability. Combustion instability is a known phenomenon in HCCI engines, discussed by Olsson et al. [14]. Olsson et al. find that HCCI combustion phasing during some circumstances drifts. This drift either causes ever earlier combustion phasing, finally damaging the engine, or ever later combustion phasing finally resulting in misfire. The factor thought to set this instability off in this case is the glass piston window which is not able to conduct heat as well as a normal steel piston. An experimental engine with piston glass is thus more prone to instability than a “normal” HCCI engine without optical access.

To explain and show the mentioned combustion instability CA50 was investigated. Figure 4 shows CA50 as it changes after a positive step disturbance and it is easily noticed that the combustion occurs earlier and earlier even about 1700 cycles after the step disturbance. Early combustion gives rise to higher peak pressure heating the engine further and the next combustion hence occurs even earlier. Finally the high peak pressure and/or the pressure oscillations caused by very early combustion will damage the engine.

MODELLING To obtain a model of the wall temperature the engine was run with the total fuel heat dictated by a Pseudo Random Binary Sequence (PRBS) [22]. Wall temperature (Figure 16) was measured and IMEP$_n$ (Figure 15) was calculated during this PRBS experiment. Since IMEP$_n$ is roughly proportional to the total fuel heat it is possible to identify a model that holds IMEP$_n$ as input and the wall temperature as output. The MATLAB® function; “n4sid” was used to perform system identification on the data collected in the experiment,“n4sid” makes use of the subspace algorithm [23].

To reduce the impact of “noise” (cyclic variability), both IMEP$_n$ and measured wall temperature were filtered using a low pass Butterworth filter. To improve the performance of the identification algorithm, mean and trend of measured wall temperature and filtered IMEP$_n$ were removed before the identification algorithm was applied. Mean and trend were removed by subtracting a first order polynomial obtained from a least-squares fit to the corresponding data. Mean and trend were then again added to the output of the model to obtain correct temperature values for the plots.

The order of the model, minimum pulse duration and duration of the PRBS experiment were selected according to *ad hoc* rules [22] based on the results of the step disturbance experiments. The minimum pulse duration was chosen as 150 engine cycles, the duration of the experiment was chosen to 4000 engine cycles (200 extra cycles are added to allow the laser to heat up). The amplitude of the PRBS signal was chosen as high as possible with the combustion instability as a limiting factor. It was possible to use an amplitude of roughly 1.7 bar IMEP$_n$. A third order model was used.

The wall temperature model obtained from the identification process is shown here below. Here $Temp_{(t)}$ is the current wall temperature, $x_{(t)}$ is the internal state of the state space model, $x_{(0)}$ are the initial state of $x_{(t)}$. The internal state of the model has no physical interpretation.

$$x_{(t+T_s)} = A * x_{(t)} + B * IMEP_{n(t)}$$
$$Temp_{(t)} = C * x_{(t)}$$

$$A = \begin{pmatrix} 0.99582 & -0.019355 & -0.004226 \\ 0.009134 & 0.80608 & -0.45149 \\ -0.0040296 & 0.16399 & -0.40477 \end{pmatrix}$$

$$B = \begin{pmatrix} 0.001359 \\ 0.041202 \\ 0.097997 \end{pmatrix}$$

$$C = \begin{pmatrix} 203.2 & -1.7954 & -0.0061066 \end{pmatrix}$$

$$x_{(0)} = \begin{pmatrix} 0.0074859 \\ -0.024105 \\ -0.028688 \end{pmatrix}$$

In order to validate the model it was used to estimate wall temperature on data from a PRBS experiment. The experimental data for the validation were not used in the system identification process, i.e. the model was cross validated against a reference data set. The result from one such cross validation can be seen in Figure 17 and Figure 18. The model is as realized from Figure 18 able to very accurately predict wall temperature. The identification and cross validation process were repeated using different sets of data and the model was always able to accurately capture the wall temperature behaviour.

DISCUSSION

The conducted experiments show that combustion chamber wall temperature has a strong impact on

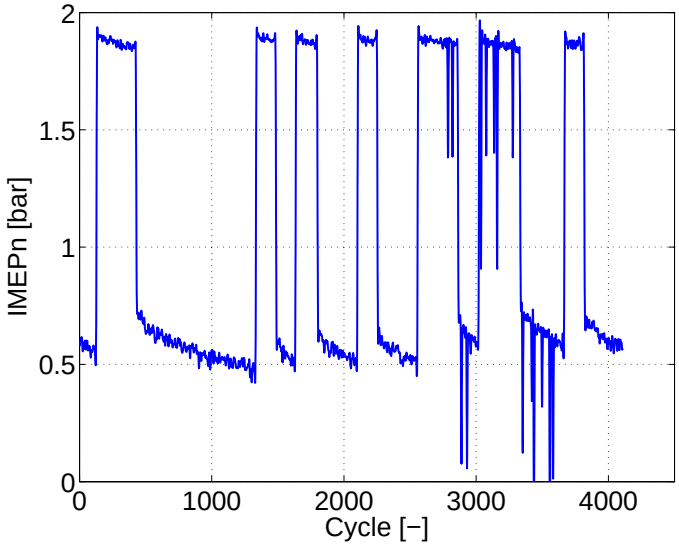

Figure 15: IMEP$_n$ PRBS experiment used in the system identification process.

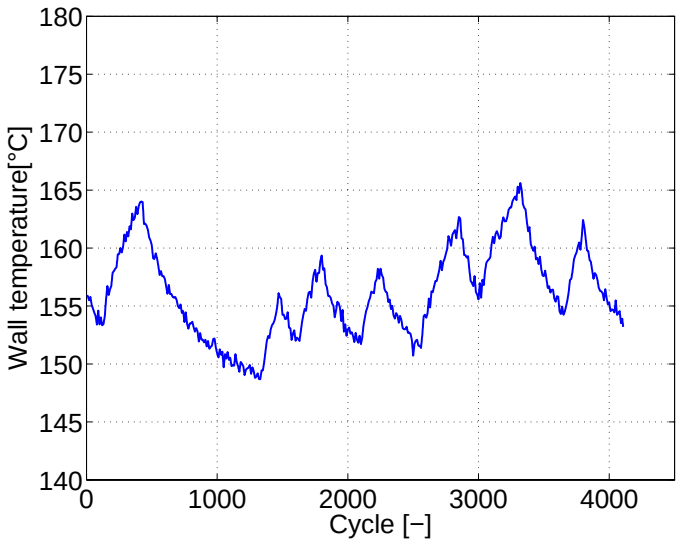

Figure 16: Measured wall temperature during the PRBS experiment used for system identification (corresponding to Figure 15).

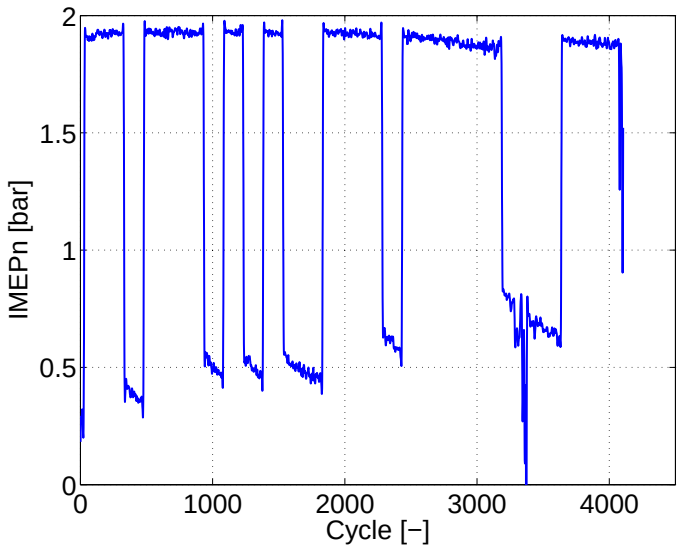

Figure 17: IMEP$_n$ PRBS sequence used in the cross validation of the state space model.

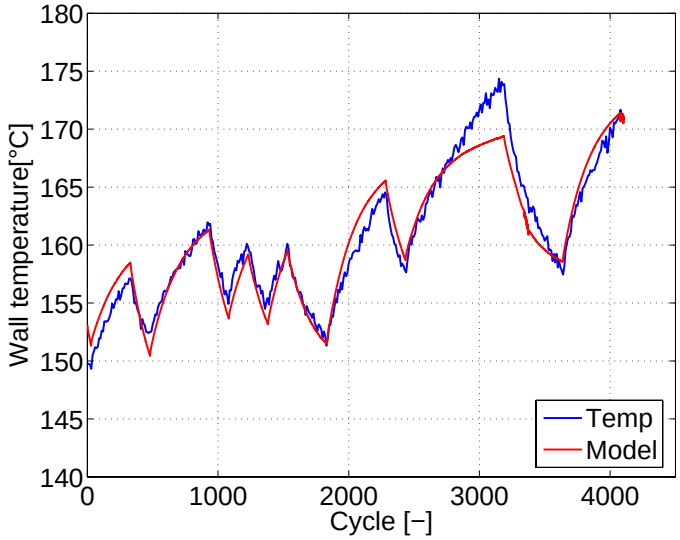

Figure 18: Cross validation, modeled and actual temperature corresponding to the sequence in Figure 17.

HCCI combustion after a sudden increase of the load. The fact that the wall temperature does not change instantaneously affects the combustion events succeeding a load transient. When load of an HCCI engine is increased, CA50 is expected to occur earlier in the cycle and combustion duration is expected to decrease. This also happens but neither the combustion duration nor CA50 changes immediately after the load has changed. The time needed for the combustion duration and CA50 to change to the new "steady state" value corresponds very well with the time it takes the combustion chamber wall to change its temperature. This implies that it is combustion chamber wall temperature that affect the combustion in terms of phasing and duration. Wall temperature change during a load transient counteracts the change of the combustion caused by a change in the load. The reason for this is that the onset of HCCI combustion is mainly governed by chemical kinetics. The chemical kinetic processes depend in turn on the combustion chamber temperature.

The rise and fall times of wall temperature are equal but the effect on combustion is different depending on if the load is increased or decreased. When load is increased wall temperature limits CA50 and combustion duration. CA50 is limited by wall temperature after a negative step disturbance as well. When load is decreased it is however the local lambda that limits combustion duration. In the negative step disturbance case, wall temperature however still affects combustion duration. After the initial change, combustion duration is slowly increasing as CA50 occurs later in the cycle.

When controlling an HCCI engine, the effect of wall temperature will cause problems during transients. Control theory contains numerous methods used to compensate a controller for a process nonlinearity (such as the wall temperature dependence). The modeling experiments show a possible method that could be used to obtain a model of the wall temperature in an engine. In the case investigated the model did accurately predict wall temperature. Since wall temperature is repetitive in its nature the model could be used to compensate for wall temperature in the combustion control. The model identified hence has the potential of simplifying transient HCCI control.

If the HCCI engine were under combustion control and if combustion phasing and duration were affected by this control, wall temperature would depend on the phasing and duration of the combustion as well. In this case when the wall temperature does not only depend on the current IMEP, a more complicated Multi Input Multi Output (MIMO) model would be needed to capture the behaviour of wall

temperature. Suitable inputs to such a MIMO wall temperature model would be IMEP, CA50 and combustion duration. The design of a MIMO model would be an interesting area of future work.

CONCLUSION

- When performing load transients in an HCCI engine the wall temperature will affect the combustion in the succeeding cycles. Combustion phasing and combustion duration depend heavily on combustion chamber wall temperature. The wall temperature shows a very slow rise time, in the conducted experiments the mean average rise time was in the range of 110 seconds.
- The wall temperature rise time equals the fall time when the increase/decrease of load is performed between the same values of IMEP.
- Repeated load step disturbances gave rise to the same rise/fall time of the combustion chamber wall temperature. This statement is valid if the combustion phasing and duration has the same initial values before the steps.
- The temperature effect on the combustion differs depending on if the disturbance is performed in positive or negative direction. When the disturbance is performed in the positive direction wall temperature has a strong and limiting effect on the combustion duration. When the disturbance is performed in the negative direction wall temperature has a very limited influence on the combustion duration. The gas properties have a much stronger impact on combustion in the negative case limiting the influence of wall temperature.
- Combustion phasing depends heavily on wall temperature both when the step disturbance is performed in the positive and in the negative direction.
- It is by the use of PRBS experiments possible to identify a state space model describing the combustion chamber wall temperature as a function of current IMEP. The model that was identified is able to accurately predict wall temperature.

REFERENCES

[1] S. Onishi, S.H. Jo, K. Shoda, P.D. Jo, S. Kato, “Active Thermo-Atmosphere Combustion (ATAC)-A New Combustion Process for Internal Combustion Engines”, SAE 790501

[2] P. Najt, D.E. Foster, “Compression-Ignited Homogeneous Charge Combustion”, SAE 830264

[3] R.H. Thring, “Homogeneous-Charge Compression-Ignition (HCCI) Engine”, SAE 892068

[4] M. Stockinger, H. Schäpertöns, P. Kuhlmann, “Versuche an einem gemischansaugenden mit Selbszündung”, MTZ 53 (1992).

[5] M. Christensen, P. Einewall, B. Johansson, “Homogeneous Charge Compression Ignition (HCCI) Using Isooctane, Ethanol and Natural Gas A Comparison to Spark Ignition Operation”, SAE 972874

[6] M. Christensen, B. Johansson, P. Amnéus, F. Mauss, “Supercharged Homogeneous Charge Compression Ignition”, SAE 980787

[7] M. Christensen, B. Johansson, “Influence of Mixture Quality on Homogeneous Charge Compression Ignition”, SAE 982454

[8] M. Christensen, B. Johansson, “Homogeneous Charge Compression Ignition with Water Injection”, SAE 1999-01-0182

[9] G. Haraldsson, J. Hyvönen, P. Tunestål, B. Johansson, “HCCI Combustion Phasing in a Multi Cylinder Engine Using Variable Compression Ratio”, SAE 2002-01-2858.

[10] J-O. Olsson, P. Tunestål, “Closed-Loop Control of an HCCI Engine”, SAE 2001-01-1031

[11] G. Haraldsson, J. Hyvönen, P. Tunestål, B. Johansson, “HCCI Combustion Phasing with Closed-Loop Combustion Control Using Variable Compression Ratio in a Multi Cylinder Engine”, SAE 2003-01-1830.

[12] J. Martinez-Frias, S. M. Aceves, D. Flowers, R. Smith, R. Dibble, “HCCI Engine Control by Thermal Management” SAE 2000-01-2869

[13] N. Milovanovic, R. Chen, J. Turner, “Influence of the Variable Valve Timing Strategy on the Control of a Homogeneous Charge Compression (HCCI) Engine” SAE 2004-01-1899

[14] J-O. Olsson, P. Tunestål, B. Johansson, S. Fiveland, R. Agama, M. Willi, D. Assanis, “Compression Ration Influence on Maximum Load of a Natural Gas Fueled HCCI Engine” SAE 2002-01-0111

[15] J. Chang, O. Güralp, Z. Filipi, D. Assanis, T-W. Kuo, P. Najt, R. Rask, “New Heat Transfer Correlation for an HCCI Engine Derived from Measurements of Instaneous Surface Heat Flux” SAE 2004-01-2996

[16] G. Särner, M. Richter, M. Aldén, A. Vressner, A. Hultqvist, B. Johansson, “Cycle to Cycle Resolved Wall Temperature Measurements using Laser-Induced Phosphorescence in an HCCI Engine”, Submitted to: SAE Powertrain & Fluid Systems Conference & Exhibition 2005, Marriott Rivercenter, San Antonio, Texas, USA

[17] T. Husberg, S. Gjirja, I. Denbratt, A. Omrane, M. Aldén, J. Engström, “Piston Temperature Measurement by Use of Thermographic Phosphors and Thermocouples in a Heavy-Duty Diesel Engine Run Under Partly Premixed Condition”, SAE 2005-01-1646

[18] A. Omrane, G. Juhlin, M. Aldén, G. Josefsson, J. Engström, T. Benham, “Demonstration of Two-Dimensional Temperature Characterization of Valves and Transparent Piston in a Gdi Optical Engine”, SAE 2004-01-0609

[19] J. S Armfield, R. L Graves, D. L. Beshears, M. R. Cates, T. V. Smith, S. W. Allison, “Phosphor Thermometry for Internal Combustion Engines”, SAE 971642

[20] S. W. Allison, G. T. Gilles, “Remote thermometry with thermographic phosphors: Instrumentation and applications”, Rev. Sci. Instrum., Vol 68, No.7, 2616, 1997

[21] Childes, Greenwood, Long, “Review of temperature measurement”, American Institute of Physics, vol 71, nr 8, 2000

[22] R. Johansson, “System Modeling and Identification”, Prentice Hall, Englewood Cliffs, NJ, 1993

[23] L. Ljung, “System Identification, Theory for the user”, Prentice Hall, 1999

[24] K. J. Åström, B. Wittenmark, “Computer-Controlled Systems”, Prentice Hall, 1997

CONTACT

Carl Wilhelmsson MSc E. E.
(e-mail: carl.wilhelmsson@vok.lth.se)
Gustaf Särner MSc
(e-mail: gustaf.sarner@forbrf.lth.se).

DEFINITIONS AND ABBREVIATIONS

CA50:	Crank angle 50% burned
CAD:	Crank Angle Degree
IMEP:	Indicated Mean Effective Pressure
IMEP_n:	Net Indicated Mean Effective Pressure
λ :	Relative air/fuel ratio
HCCI:	Homogeneous Charge Compression Ignition
HR:	Heat Release
PFI:	Port Fuel Injection
PRBS:	Pseudo Random Binary Sequence
TDC:	Top Dead Center
BDC:	Bottom Dead Center
BBDC:	Before Bottom Dead Center
BTDC:	Before Top Dead Center
ATDC:	After Top Dead Center
MIMO:	Multiple Input Multiple Output